

## Optical generation of matter qubit graph states

S C Benjamin<sup>1</sup>, J Eisert<sup>2,3</sup> and T M Stace<sup>4</sup>

<sup>1</sup> Materials Department, University of Oxford, Oxford OX1 3PH, UK

<sup>2</sup> Quantum Optics and Laser Science, Blackett Laboratory,  
Imperial College London, London SW7 2BW, UK

<sup>3</sup> Institute for Mathematical Sciences, Imperial College London,  
London SW7 2BW, UK

<sup>4</sup> Department of Applied Mathematics and Theoretical Physics,  
University of Cambridge, Cambridge CB3 0WA, UK

E-mail: [simon.benjamin@materials.oxford.ac.uk](mailto:simon.benjamin@materials.oxford.ac.uk)

*New Journal of Physics* **7** (2005) 194

Received 21 June 2005

Published 16 September 2005

Online at <http://www.njp.org/>

doi:10.1088/1367-2630/7/1/194

**Abstract.** We present a scheme for rapidly entangling matter qubits in order to create graph states for one-way quantum computing. The qubits can be simple three-level systems in separate cavities. Coupling involves only local fields and a static (unswitched) linear optics network. Fusion of graph-state sections occurs with, in principle, zero probability of damaging the nascent graph state. We avoid the finite thresholds of other schemes by operating on two entangled pairs, so that each generates exactly one photon. We do not require the relatively slow single qubit local flips to be applied during the growth phase: growth of the graph state can then become a purely optical process. The scheme naturally generates graph states with vertices of high degree and so is easily able to construct minimal graph states, with consequent resource savings. The most efficient approach will be to create new graph-state edges even as qubits elsewhere are measured, in a ‘just in time’ approach. An error analysis indicates that the scheme is relatively robust against imperfections in the apparatus.

**Contents**

<b>1. Introduction</b>	<b>2</b>
<b>2. Graph states and cluster states</b>	<b>4</b>
<b>3. Description of the physical scheme</b>	<b>5</b>
3.1. Physical components . . . . .	5
3.2. Action on product states . . . . .	7
3.3. Fusion of graph states . . . . .	7
3.4. Growing a graph state without employing local gates . . . . .	9
3.5. Further remarks on graph growth . . . . .	11
<b>4. Characteristics of the derived graph states</b>	<b>11</b>
4.1. MGS . . . . .	11
4.2. Generation of edges . . . . .	11
4.3. Cluster states . . . . .	12
<b>5. Just in time graph creation</b>	<b>14</b>
<b>6. Error analysis</b>	<b>14</b>
6.1. Continuous measurement analysis . . . . .	15
6.2. Photon loss . . . . .	17
6.3. Other errors . . . . .	18
<b>7. Summary</b>	<b>19</b>
<b>Acknowledgments</b>	<b>19</b>
<b>References</b>	<b>19</b>

**1. Introduction**

Despite significant and exciting experimental progress in recent years, the physical realization of a full-scale quantum computer (QC) remains a tremendous challenge [1]. In many systems excellent single qubits have already been realized (notably, of ions in a trap [2, 3], NV (nitrogen vacancy) centres in diamond [4, 5], etc). However, few systems have demonstrated controlled qubit–qubit coupling between pairs taken from more than four qubits, and achieving the necessary exquisite control remains highly problematic. In general, it is difficult to simultaneously satisfy the two key requirements of coupling different subsystems in a controlled manner, while at the same time shielding the system from its environment [1]. In the majority of QC schemes, some direct physical interactions are supposed to generate the two-qubit operations (e.g. phonon modes among trapped ions [2, 3], Förster interactions between excitations in semiconduction quantum dots [6], etc). Thus, one calls for the qubits to strongly interact with selective parts of their environment (namely, other qubits and the control mechanisms), while avoiding interactions with the rest of the environment to a near perfect degree. This is obviously a challenging prescription.

As an alternative to employing a direct physical interaction between qubits, one can exploit the entangling power of measurements. A suitable measurement, at least for certain outcomes, will have the effect of projecting previously separate qubits into a highly entangled state. This idea has been explored as a route to QC using photon qubits in a linear optical apparatus. Measurement-based gates have indeed been shown to be sufficient for universal gate-based

quantum computation [7]. However, in order to achieve each logical gate with high probability, one must prepare and then consume large auxiliary resources. This necessity is essentially due to the small probability of success of the elementary quantum gates based on auxiliary systems and measurements [8].

One way to reduce this overhead is to exploit the idea of one-way computing [9, 10]. In this approach, one would prepare a certain multi-qubit entangled state, a cluster [9] or a graph state [10, 11], prior to the computation. This state has the property that the computation can then proceed purely by single-qubit measurement—essentially consuming the graph entanglement as a resource. Recently, there has been a successful proof-of-principle experiment realizing a four-qubit cluster state [12]. A key advantage of the one-way computing strategy is that it introduces a degree of separation between the act of creating entanglement and the act of executing the computation. Thus, we need not expend the effort needed to ensure that each entangling operation succeeds with high probability—we can tolerate failures during the growth process simply by rebuilding the affected graph section, provided of course that failures are ‘heralded’. Indeed, in this spirit, various recent schemes [13]–[15] have shown how to take gate operations that are fundamentally non-deterministic, and use them to construct as such an entangled resource state with certainty.

One particularly attractive possibility is to use matter qubits, with the obvious benefits that they are static and potentially long lived, together with an optical coupling mechanism that creates suitable entanglement. Based on earlier schemes that allow for generating entanglement or realizing quantum gates in matter qubits using flying optical qubits [16]–[23], two recent publications [24, 25], in particular, have explored precisely this possibility. The matter qubits can be completely separate, for example each within its own cavity apparatus, providing that suitable optical channels connect them to a mutual measurement apparatus. The simplest scheme is that of Barrett and Kok (BK) [24], where one requires only a single-beam splitter and two detectors in order to couple pairs of qubits. The elegant BK approach, however, suffers from the constraint that, even with ideal apparatus, the entangling operation must fail with a probability of  $p = 1/2$ . Failures damage the nascent graph state, but because the failure is flagged, or ‘heralded’, the damaged parts can be removed and the growth can continue. Nevertheless, the high rate of destructive failures introduces a considerable overhead [26], especially with certain types of target graph topology. The scheme due to Lim, Beige and Kwek (LBK) [25] introduces the idea of ‘repeat until success’ entanglement, meaning that while failures still occur with probability  $p \geq 1/2$ , these failures are essentially passive and one can simply try again. Thus, one can construct graph states with a lower overhead, in terms of number of entangling operations, and any topology can be directly implemented. However, the cost for this advance is that the underlying coupling process is more complex: each matter qubit gives rise to a superposition of an ‘early’ and a ‘late’ photon in time-bin encoding, which must subsequently enter a beam splitter apparatus simultaneously. This appears to be more challenging relative to the simpler BK scheme, so that it is an open question, which scheme is the more practical.

Here, our goal is to unite the more desirable features of both these schemes, in particular the simple static optical apparatus of the BK scheme and the non-destructive ‘repeat-until-success’ aspect of the LBK approach. Moreover, we introduce a vital feature which neither of these approaches possess: we demonstrate a graph growth mechanism which does not require local unitary operations (e.g. flips) to be performed on the matter qubits during the growth process. The growth then becomes purely a sequence of optical excitations, with a corresponding significant increase in speed and considerable reduction in complexity.

We intend that the present paper will form a self-contained overview of the entire paradigm that we are advocating, and to this end we include compact analysis of the relevant properties of graph states. We make use of the idea of a minimal graph state (MGS), and make a comparison with the more limited ‘cluster states’ which results when the geometry of physical qubits and their neighbours are fixed by experimental constraints. We conclude that there are dramatic savings, in terms of qubits and entangling operations, when one adopts an architecture that can build an MGS directly.

## 2. Graph states and cluster states

Graph states [10, 11, 27] are multi-qubit entangled states, which can be conceived as having been entangled according to certain pattern of two-qubit phase gates. Formally, this pattern is specified by the adjacency matrix of an (undirected simple) graph  $G(V, E)$ , where  $V$  denotes a set of  $n$  vertices associated with the qubits, and edge set  $E$  reflecting the phase gates (see figure 1(d) for example). The graph state of the empty graph has the state vector  $|\Psi\rangle = |+\rangle^{\otimes n} = ((|0\rangle + |1\rangle)/\sqrt{2})^{\otimes n}$ . The state vector of a graph state including edges can then be written as

$$|G\rangle = \prod_{(a,b) \in E} P^{(a,b)} |+\rangle^{\otimes n}, \quad (1)$$

with  $P^{(a,b)}$  corresponding to a phase gate  $P^{(a,b)} = (\mathbb{1} + \sigma_z^{(a)} + \sigma_z^{(b)} - \sigma_z^{(a)} \otimes \sigma_z^{(b)})/2$  between qubits labelled  $a$  and  $b$ , expressed in terms of Pauli operators. Such graph states are stabilizer states<sup>5</sup>, and in turn, every stabilizer state of  $n$  qubits is locally equivalent to a graph state [28, 29].

A cluster state (CS) [9] is a particular graph state: it is one with an underlying cubic lattice of one, two or three dimensions (see figure 2(a) for example). A cluster state of more than one dimension has the remarkable property that it forms a universal resource for measurement-based one-way computing: having created this state, the actual computation is executed simply by making local measurements [9, 10]. It is universal in the sense that the procedure amounts to effectively implementing an arbitrary unitary on the input qubits.

However, the measurements performed in order to implement some chosen algorithm will include two classes which it is important to distinguish [9, 10]. The first are the Pauli measurements, which we can denote as measurements along the  $X$ ,  $Y$  or  $Z$  axis. Each such measurement maps a graph state onto another graph state for all outcomes. For example, the  $Z$  measurement effectively deletes the measured qubit (node) and its associated edges, while  $X$  and  $Y$  measurements alter the graph according to the rules given in [11]. These measurements correspond to the Clifford-part of the computation, and the resulting map on the level of states can always efficiently be determined on a classical computer [10]. Having performed all the prescribed Pauli measurements on a cluster, we are left with an MGS which is the graph containing the smallest number qubits that is capable of realizing our desired algorithm.

<sup>5</sup> Its stabilizer is given by the Abelian group generated by the mutually commuting operators

$$K_a = \sigma_x^{(a)} \prod_{b \in N_a} \sigma_z^{(b)}, \quad (2)$$

$N_a$  denoting the set of neighbours of  $a$ .

The remaining measurements are of the second class: von Neumann measurements in tilted bases. Such measurements take the system out of the graph-state prescription and generally cannot be efficiently simulated on a classical computer. In a sense one can think of the Pauli measurements as simply customizing the (initially universal) cluster state into the form that will implement our chosen algorithm, while the more general tilted measurements actually execute the algorithm.

Many physical systems that can generate graph states are in fact limited to cluster state generation, because the physical qubit interactions are limited to some kind of nearest-neighbour (or at any rate, local) form. This applies to implementations in electron spin lattices and optical lattices. However, we are under no such constraint since the physical qubits have no defined geometry<sup>6</sup>. Instead, we can directly ‘grow’ an arbitrary graph, and hence we may prepare the graph state that forms the specific resource for a given quantum algorithm. We would therefore seek to directly build an MGS, shortcutting the creation of the cluster state with its redundant universality. This proves to have dramatic advantages in terms of the number of entanglement operations and qubits needed. In general, one finds that an MGS will often exhibit a high vertex degree, and will contain significantly fewer qubits compared to the graph state that is obtained from a cluster state after measurements along the Z basis, essentially merely removing qubits (typically up to an order of magnitude). Explicit examples are described later.

### 3. Description of the physical scheme

In this section, we describe the physical requirements and processes involved in implementing our proposal. We start by describing the elementary physical systems required. We then outline the action of the beam-splitter network, both on simple product states and more importantly when fusing graph states together. Finally, we then show how to do this without any single-qubit unitary, and make some concluding comments.

#### 3.1. Physical components

In figure 1(a), we indicate the basic energy level scheme that our matter qubits should incorporate. Obviously, a real quantum system may have additional levels, provided these three-level dynamics are incorporated, then such a system is suitable. Candidates include an actual atom or ion in a trap, of course, but we may also consider any optically active solid-state structure with a discrete spectrum, such as a quantum dot, or NV-diamond centre [38]. The ground states, labelled with state vectors  $|0\rangle$ ,  $|1\rangle$ , are the qubit basis states. The third level, labelled  $|e\rangle$ , provides a mechanism for producing a photon from the atom, conditional on the atom being in state labelled with state vector  $|1\rangle$ . That is, there is an externally driven transition from  $|1\rangle \rightarrow |e\rangle$  by using a  $\pi$ -pulse, followed by the optical relaxation  $|e\rangle \rightarrow |1\rangle$  which emits a single photon into the cavity mode, and eventually ‘leaks’ out to an external optical network. In a single-mode description, this is characterized by a coupling strength  $\Omega$  of the Jaynes–Cummings coupling between the transition  $|1\rangle \rightarrow |e\rangle$  and the cavity mode, with decay rate  $\Gamma$  of the cavity mode. The

<sup>6</sup> In optical lattices, graph-state preparation has been considered in [30, 31]. A promising sequential generation of multi-qubit matrix-product states—and hence also cluster states—in time-bin encoding using optical cavities has in turn been considered in [32].

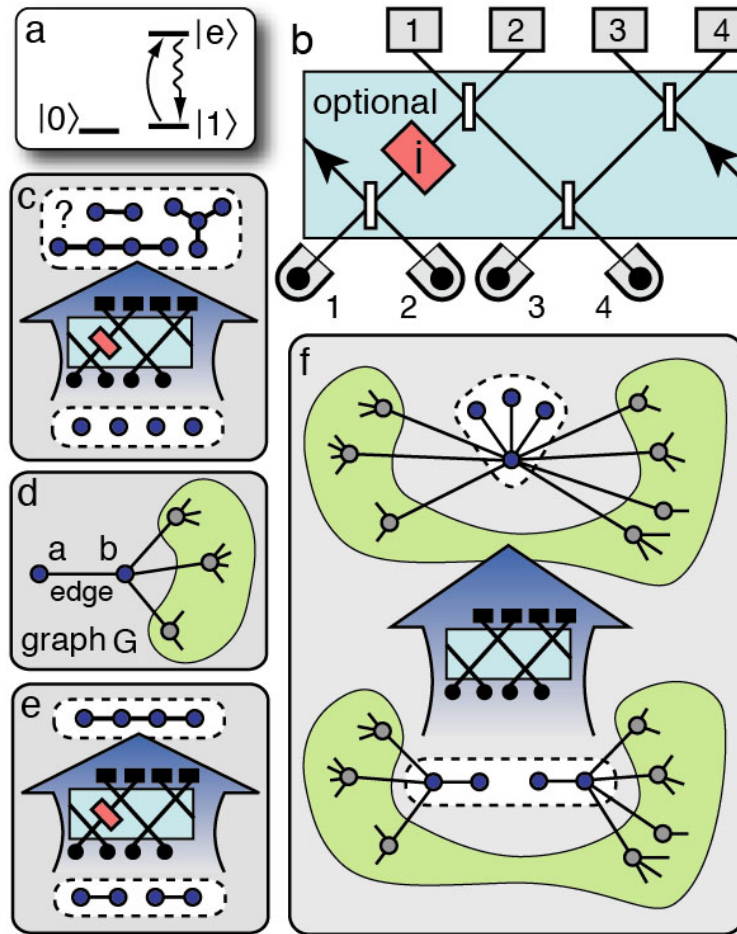


**Figure 1.** (a) The energy level scheme for a matter qubit. (b) Our apparatus: matter qubits  $j = 1, \dots, 4$  (lower) emit photons to detectors  $k = 1, \dots, 4$  (upper) via beamsplitters. We consider two variants of the device: one with a phase shifter as marked, one without. (c) The effect of excitation and measurement when four product state qubits are employed—there are various possible results depending on the number and pattern of detected photons. (d) A graph state in which a ‘leaf’ qubit, marked ‘b’, is attached by only one edge. (e) The effect of applying our protocol (with shifter) to two EPR pairs. (f) The effect of applying our protocol (without shifter) to two arbitrary graphs as shown.

system is continuously observed via the photon detectors placed behind the four beam-splitter array (4BS). We note that, as remarked in [25], if we have a fourth level accessible from  $|e\rangle$ , then we can potentially create a photon directly in the cavity without significantly populating  $|e\rangle$ —this may be advantageous in avoiding dephasing. The state labelled  $|e\rangle$  is also exploited when we wish to make a measurement—continuous illumination by a laser adjusted to the transition energy will result in a fluorescence, conditional on the qubit state. This is a Z measurement; measurement in the other directions is accomplished by an appropriate local rotation followed by this fluorescence.



The elementary multi-qubit operation in our proposal is based on a four-port beam splitter, which is a composite of four ordinary beam splitters, arranged so that every input crosses all other, and finally incident on photon counters. Two types of 4BS will be employed: one without additional phase shifts, the ‘basic network’, and one which includes a certain phase-shift corresponding to a factor of  $e^{i\pi/2}$ , the ‘shifter network’, for producing certain important cluster states. The action of the 4BS is essentially to ‘erase’ information about which cavity a photon originated from, so that a given detector cannot differentiate between matter qubits. Ideally the frequencies of the modes are identical, and other sources of mode matching problems are to a high extent eliminated—we analyse the effects of realistic imperfections in section 6.

### 3.2. Action on product states

The analysis to determine the specific projections is straightforward. The most simple interesting case we examine is that of inputting four qubits in the product state corresponding to  $|+\rangle^{\otimes 4}$ . The action of the optical excitation  $|1\rangle \rightarrow |e\rangle$  applied to all qubits, followed by the emission into their local cavities, then results in an equal superposition of all basis vectors containing all binary words

$$|\phi\rangle = \frac{1}{4} \sum_{i,j,k,l=0}^1 |i, j, k, l\rangle (c_1^\dagger)^i (c_2^\dagger)^j (c_3^\dagger)^k (c_4^\dagger)^l |0\rangle, \quad (3)$$

where the annihilation operators of the respective cavity modes are denoted by  $c_1, \dots, c_4$ .

As the photons propagate through a beam splitter into new modes, we employ mappings such as  $(d_j^\dagger, d_k^\dagger)^T = B(c_j^\dagger, c_k^\dagger)^T$ ,  $j, k = 1, \dots, 4$ , where phases of the transmitted and reflected modes are chosen such that  $B$  is given by

$$B = \frac{1}{\sqrt{2}} \begin{pmatrix} 1 & i \\ i & 1 \end{pmatrix}. \quad (4)$$

Thus, the network corresponds to a unitary manipulation of the photon states. In this way, we eventually obtain the final generation of operators representing photons in the modes upon which the detectors act. Thus, we determine the state that results from a particular detector reading. In fact, a number of states can occur, including states that are locally equivalent to linear four-qubit graphs and three-nodes, as shown in figure 1(c).

### 3.3. Fusion of graph states

The ability to generate such graphs directly from product states appears to be a promising characteristic. However, to properly differentiate the possible outcomes, one would require either resolving photon detectors (capable of distinguishing a single photon from a pair, etc) or else one would need to resort to a lengthy asymptotic variant of the ‘double heralding’ idea in [24]. These undesirable features result from the fact that the system’s state, prior to photon measurement, was not an eigenstate of the total photon number operator: there are elements in the superposition corresponding to 0,  $\dots$ , 4 photons. To avoid the problem, we must contrive to introduce a known number of photons. This is the same issue faced in [25], where the authors suggest resorting to time-bin approach and local flips in order to guarantee that each matter qubit ultimately generates one photon.

We take a different route, based on the idea of ‘fusing’ graphs together. We will find that we can regard EPR pairs as a kind of raw ingredient from which graphs of arbitrary complexity can be grown deterministically. Recall that an EPR pair with state vector  $|\text{EPR}\rangle = (|0, 1\rangle - |1, 0\rangle)/\sqrt{2}$  is already LU-equivalent to the simplest non-trivial graph state, the one consisting of two vertices connected by an edge. We use the term ‘LU-equivalent’ to mean, equivalent up to local unitary operations on individual qubits. Our fusion process exploits existing entanglement within the graphs sections: certain vertex pairs within a graph state can be locally rotated to the subspace  $\text{span}\{|0, 1\rangle, |1, 0\rangle\}$ —two such pairs then generate precisely two photons.

Suppose that a ‘leaf’ node exists, i.e. a certain vertex (associated with qubit  $a$ ) is attached to only one other vertex (associated with qubit  $b$ ) of the graph. This is shown in figure 1(d). Then the state vector  $|\Psi_G\rangle$  of the entire graph state is of the following form

$$|\Psi_G\rangle = (|0, 0\rangle + |1, 0\rangle + |0, 1\rangle P - |1, 1\rangle P)|\psi\rangle, \quad (5)$$

where the vectors  $|a, b\rangle$  correspond to the qubits  $a, b$ , and  $|\psi\rangle$  refers to the external, arbitrarily connected part of the graph state, shown inside the green bubble in figure 1(d). We define

$$P = \prod_{i \in N_b \setminus \{a\}} \sigma_z^{(i)}, \quad (6)$$

so with index  $i$  running over the neighbours  $N_b$  of qubit  $b$  lying within  $|\psi\rangle$ . This state vector is in turn equivalent, up to a unitary rotation  $(\mathbb{1} - i\sigma_y^{(a)})/\sqrt{2}$  on  $a$ , to

$$|\Psi_E\rangle = (|1, 0\rangle + |0, 1\rangle P)|\psi\rangle. \quad (7)$$

Having made this transformation, we know that our qubit pair labelled  $a$  and  $b$  will emit precisely one photon. If we similarly prepare a second pair of qubits, associated with a different graph (or, a different part of the same graph) then the two pairs of qubits can be employed in our 4BS device and will generate precisely two photons. As indicated in figure 1, we have considered two variants of the beam-splitter network: one with and one without a phase shifter. A simple analysis determines that in both cases there are two possible classes of outcome. The two photons may arrive in a single detector, in which case the effect is simply equivalent to applying local phase gates to the matter qubits. Alternatively, the two photons may enter different detectors, in which case the two pieces of graph are fused together in a fashion we specify presently. Identifying the various outcomes does not require counting photon detectors, since we know there are two photons in total (but such detectors may be useful in fighting errors when taking imperfections into account, see section 6).

The two classes of outcome are equally probable. In the case of the former, one can try again without pausing to correct the local phases, which can be fixed after the eventual successful fusion. The average number of attempts required is two. This is then a ‘repeat-until-success’ scenario equivalent to the one first observed in [25]. The particular form for our fused graph depends on whether the phase shifter was employed. If we do employ the shifter, and supposing that we input two EPR pairs, then the resulting state is LU-equivalent to a linear four-qubit graph as shown in figure 1(e). If instead we use our 4BS without the phase shifter, i.e. the basic network, we can couple arbitrary graph fragments according to the rule shown in figure 1(f). For the example



**Table 1.** State vectors resulting from clicks in detectors  $k_1$  and  $k_2$ , and their probabilities, for the basic beam-splitter network acting on the state  $|\text{EPR}\rangle_{1,2}|\text{EPR}\rangle_{3,4}$ , where  $|a\rangle = (|0, 1\rangle + i|1, 0\rangle)(|0, 1\rangle - i|1, 0\rangle)/2$ ,  $|b\rangle = (|0, 1\rangle - i|1, 0\rangle)(|0, 1\rangle + i|1, 0\rangle)/2$ ,  $|c\rangle = (|0, 1, 0, 1\rangle - |1, 0, 1, 0\rangle)/\sqrt{2}$ ,  $|d\rangle = (|0, 1, 1, 0\rangle + |1, 0, 0, 1\rangle)/\sqrt{2}$ . State vectors  $|c\rangle$  and  $|d\rangle$  are LU-equivalent to a graph-state vector in which a central vertex radiates three ‘leaf’ vertices.

$ \Psi(k_1; k_2)\rangle$ ; Prob	1	2	3	4
1	$ a\rangle; \frac{1}{8}$	0; 0	$ c\rangle; \frac{1}{16}$	$ d\rangle; \frac{1}{16}$
2	0; 0	$ a\rangle; \frac{1}{8}$	$ d\rangle; \frac{1}{16}$	$ c\rangle; \frac{1}{16}$
3	$ c\rangle; \frac{1}{16}$	$ d\rangle; \frac{1}{16}$	$ b\rangle; \frac{1}{8}$	0; 0
4	$ d\rangle; \frac{1}{16}$	$ c\rangle; \frac{1}{16}$	0; 0	$ b\rangle; \frac{1}{8}$

of joining two EPR states, we show the outcome states conditioned on which detectors click, and their probabilities in table 1. These observations lead us to regard EPR pairs as the basic resource for graph growth: EPR pairs can be generated easily by a single-beam splitter using the BK scheme, or equivalently we have observed that they can be obtained from our 4BS network by choosing to excite just two of the four qubits. The combination of the two coupling processes (figures 1(e) and (f)) then allows graphs of arbitrary complexity to be built. Recall that a graph can be ‘pruned’, i.e. qubit nodes can simply be removed, by making a Z axis measurement, while other useful transforms result from X or Y measurements [11]. Indeed, a recent preprint [39] makes ingenious use of measurements on leaf structures, reminiscent of those occurring at the fusion point in figure 1(f), for qubit loss tolerance in graph states.

### 3.4. Growing a graph state without employing local gates

We have seen that we can grow graphs by transforming selected qubits to an EPR-type basis prior to fusion, and then applying additional LU operations to transform the ‘raw’ resultant state back to a graph state. But, can we avoid these local transformations? It is evidently necessary to employ single-qubit rotations at two stages: the very beginning in the entangling procedure, where we must take ‘fresh’ qubits and prepare them in  $|+\rangle$  in order to synthesize the EPR pairs which we regard as our basic ingredient, and the very end where we will wish to rotate qubits prior to our fluorescence measurement, in order to synthesize measurements along some general axis. Remarkably, we can in fact omit the numerous local rotations during graph-state growth. We find that, within a light constraint on the growth process, we can ensure the state remains LU-equivalent to a graph state at each growth step.

To see that this is possible consider the following argument. Suppose that we have some multi-qubit state vector  $|\Psi\rangle$  which meets the following two conditions:

- (i) The state vector  $|\Psi\rangle$  is equivalent up to local unitary operations to  $|\Psi_G\rangle$  corresponding to a graph  $G$  of the form as in figure 1(d).
- (ii) Regarding the pair of qubits labelled  $a$  and  $b$ ,

$$|\langle 0, 1|\Psi\rangle| = |\langle 1, 0|\Psi\rangle|, \quad |\langle 0, 0|\Psi\rangle| = |\langle 1, 1|\Psi\rangle| = 0. \quad (8)$$

From (i) and recalling equation (7), we know that  $|\Psi\rangle$  is LU-equivalent to a state vector  $|\Psi_E\rangle = (|1, 0\rangle + |0, 1\rangle P)|\psi\rangle$  since that is itself LU-equivalent to the graph-state vector corresponding to  $G$ . The additional constraint (ii) implies that our state vector can be written as

$$|\Psi\rangle = (|1, 0\rangle U + |0, 1\rangle \tilde{U})|\psi\rangle, \quad (9)$$

where  $U$  is a product of local unitaries acting on  $|\psi\rangle$ , i.e. acting in the Hilbert spaces of the qubits other than those labelled  $a$  and  $b$ , and  $\tilde{U} = \exp(i\phi)UP$  with  $\phi \in [0, 2\pi)$  an arbitrary phase. Now let us apply the 4BS process of figure 1(f) to  $a$  and  $b$ , along with an equivalent pair from some analogous graph state (or, another part of the same graph state). On failure (with probability  $1/2$ ), the process simply introduces some known local phases, which do not alter our prescription. On eventual success, we generate a state vector

$$|\Psi_{\text{tot}}\rangle = (|X\rangle U_{\text{tot}} + |\bar{X}\rangle \tilde{U}_{\text{tot}})|\psi_{\text{tot}}\rangle. \quad (10)$$

Here,  $X$  is a binary word with two zeros, two ones, and  $\bar{X}$  is its complement. The vector  $|\Psi_{\text{tot}}\rangle$  refers to the entire state vector of the fused system, and  $|\psi_{\text{tot}}\rangle$  is the state vector for all qubits except the four that coupled via the 4BS. Similarly,  $U_{\text{tot}}$  is some product of local unitaries on  $|\psi_{\text{tot}}\rangle$  and  $\tilde{U}_{\text{tot}} = e^{i\theta} P_{\text{tot}} U_{\text{tot}}$ , where

$$P_{\text{tot}} = \prod_i \sigma_z^{(i)} \quad (11)$$

with the index running over neighbours of either of the original vertices (but excluding mutual neighbours). The phase  $\theta \in [0, 2\pi)$  is determined by  $\phi$  and its counterpart in the second pair, together with phases introduced in any failure preceding the successful fusion. This state vector  $|\Psi_{\text{tot}}\rangle$  is indeed LU-equivalent to the desired fused graph state of figure 1(f). Moreover, because  $X$  has two zeros and two ones, if we nominate one of those four qubits to be a new ‘vertex’ qubit  $b$ , two of the three remaining ‘leaf’ qubits are available to be labelled as  $a$  to satisfy (i) and (ii). Thus, we can go on to perform further fusions using  $|\Psi_{\text{tot}}\rangle$ . To conclude the argument, we need to only observe that conditions (i) and (ii) are met by simple EPR pairs, and by the state resulting from fusing two EPR pairs via the process depicted in figure 1(e), i.e. the state that is LU-equivalent to a linear four-qubit graph state. Thus, these simple states can act as the initial building blocks as we construct a complex graph.

We can grow our entire graph from EPR pairs without the use of local unitary operations during the growth process, provided we are prepared to measure out one in every three of the ‘leaf’ nodes which occur at each fusion point. This constraint is extremely light: we would rarely wish to use all three leaves, and in any case the number of leaves can be increased by two, simply by fusing an EPR pair, which adds one to the number of leaves that are eligible in the sense of property (ii). Of course, the LU operations needed to map the final state to the desired ultimate graph state can subsumed into the rotation which in any case precedes measurement. The growth process is therefore entirely one of optical excitation and detector monitoring. One can anticipate that in many systems, the cost in efficiency arising from following the constraint would be vastly outweighed by the increase in growth speed.

### 3.5. Further remarks on graph growth

There is one additional comment to make regarding the speed of our protocol: in the scheme from [24] it is always necessary to wait a period after the initial measurement to ensure there are no further photons in the apparatus. The fidelity of the entangled states is only high if this wait period is long compared to the typical time for a photon to be detected. This additional waiting time necessary in [24] is not necessarily long, given that photon emission from these sources is approximately exponential, governed by the timescale  $1/\Gamma_{\text{slow}}$ . By contrast, because we contrive to have precisely two photons in the apparatus, once we see two detection events (either in different detectors, or, given resolving detectors as discussed later, within one detector) we have no need for such a wait. One should hence expect a factor of about 5 in difference concerning the speed of this step in the respective schemes.

In a mature form of the architecture described here, one would envisage coupling the many qubits by a form of  $N$ -port all-optical router, as used in integrated optics, so that our qubits can remain static and we can choose which of them will couple by suitably setting the router and optically exciting only that subset. Devices relevant to this technology have already been developed for classical optical communications [33]. This would permit direct growth of graphs with an arbitrary topology, and in particular the ability to directly entangle arbitrary qubits gives a non-local architecture [34]–[36]. Such non-local architectures may prove to have an advantage in quantum fault tolerance and error correction [37].

## 4. Characteristics of the derived graph states

As discussed above and illustrated in figure 1, our protocol can generate graphs of arbitrary topology, including nodes of high degree. We argued earlier in section 2 that, given such an architecture, one should aim to create MGS. The advantage in terms of resource consumption when preparing appropriate MGS compared to standard cluster states (CS) can be quite significant.

### 4.1. MGS

In the best-known scheme for an  $n$ -qubit quantum Fourier transformation [10], the number of required qubits is  $C_{\text{Fourier}}(n) = 8n^2 + O(n)$  for a cubic cluster, followed by first  $X$ ,  $Y$  and  $Z$  measurements, then tilted measurements. The MGS embodies  $G_{\text{Fourier}}(n) = (3/2)n^2 + O(n)$  qubits. In turn, for the quantum adder [10],

$$C_{\text{Adder}}(n) = 312n + O(1), \quad G_{\text{Adder}}(n) = 16n + O(1). \quad (12)$$

Hence, one may gain more than an order of magnitude in resource consumption. For the three-qubit Toffoli gate that we use here as our illustration, we have  $G_{\text{Toffoli}} = 13$  versus  $C_{\text{Toffoli}} = 65$ , such that there is a factor of 5 difference in the number of qubits.

### 4.2. Generation of edges

Concerning the actual preparation of the graph states, we emphasize two points: firstly, when introducing edges with a physical interaction, one should always prepare the LU-equivalent graph

state corresponding to the graph with the minimal number of edges. Or, more specifically, the graph state with the minimal number of edges that is equivalent up to local Clifford unitaries<sup>7</sup>, which merely amount to a local Clifford basis change. This has also been emphasized in [42]. Fortunately, an efficient algorithm is known to check full local Clifford equivalence [43]. Any graph that corresponds to local Clifford equivalent graph states can be related to each other with a successive application of local complementations [11, 43]. Also, it is known how many different graph states are contained in an equivalence class with respect to local Clifford unitaries [28].

Secondly, the present scheme seems particularly suitable to prepare graph states of graphs involving vertices with a high vertex degree in a single step. In a CS after measurement of the unused qubits along the Z direction, it suffices to have vertices with a maximal vertex degree of 3. This is obviously the lowest possible for a graph less trivial than a linear cluster state. From the example of figure 2, one would suspect that a typical MGS may need higher degree nodes, and this is an important question in considering how they can be efficiently constructed. To explore this point, we consider the ‘maximal vertex degree’, by which we mean, the highest degree of any vertex in the graph. The vertex degree in an MGS can in principle take any value. The maximal vertex degree is notably not invariant under local Clifford unitaries (see footnote 7). To render the notion of maximal vertex degree meaningful, we have to take its minimum value when minimized over all local Clifford unitaries. For a GHZ state of  $n$  qubits, it can easily be shown that it has a smallest maximal vertex degree of  $n - 1$ . So we immediately see that it is meaningful to talk about ‘highly connected graph states’. For the resource state for the [7,1,3]-CSS code as considered in [11], we find that in the whole orbit under local Clifford unitaries the smallest maximal vertex degree is 6, whereas the largest is 34. In the three-qubit quantum Fourier transform the smallest maximal vertex degree is 4. Thus, we see that high degree vertices are indeed generally unavoidable in an MGS: any scheme that claims to be able to directly and efficiently construct such a state must be able to create graph states with vertices of high vertex degree. The BK scheme, for example, appears somewhat limited by the increased difficulty of making the high degree vertices associated with graph states; the high rate of destructive failures leads one to take an indirect approach as depicted in figure 2(e), with an associated cost in resources. The scheme presented here is among the few that generate high-degree nodes directly (see footnote 6), as one can quickly see by considering the fusion rule depicted in figure 1(f).

#### 4.3. Cluster states

Of course, if for some reason we wished to generate a conventional CS rather than the MGS specific to some given algorithm, then we can do so efficiently. As an exercise, let us conclude this section with a comment on the required number of steps in the preparation of a CS with an underlying two-dimensional cubic lattice. We will count resources in terms of the number of applications of the shifter  $N_{\text{Shifter}}$ , with two EPR pairs fed in at each instance, and of the basic

<sup>7</sup> It is an open problem whether to consider local Clifford unitaries is a restriction of generality when asking whether two graph states are LU-equivalent. In a large number of cases for  $n$  qubit graph states, one can show that it indeed suffices to take Clifford unitaries into account [40, 41].

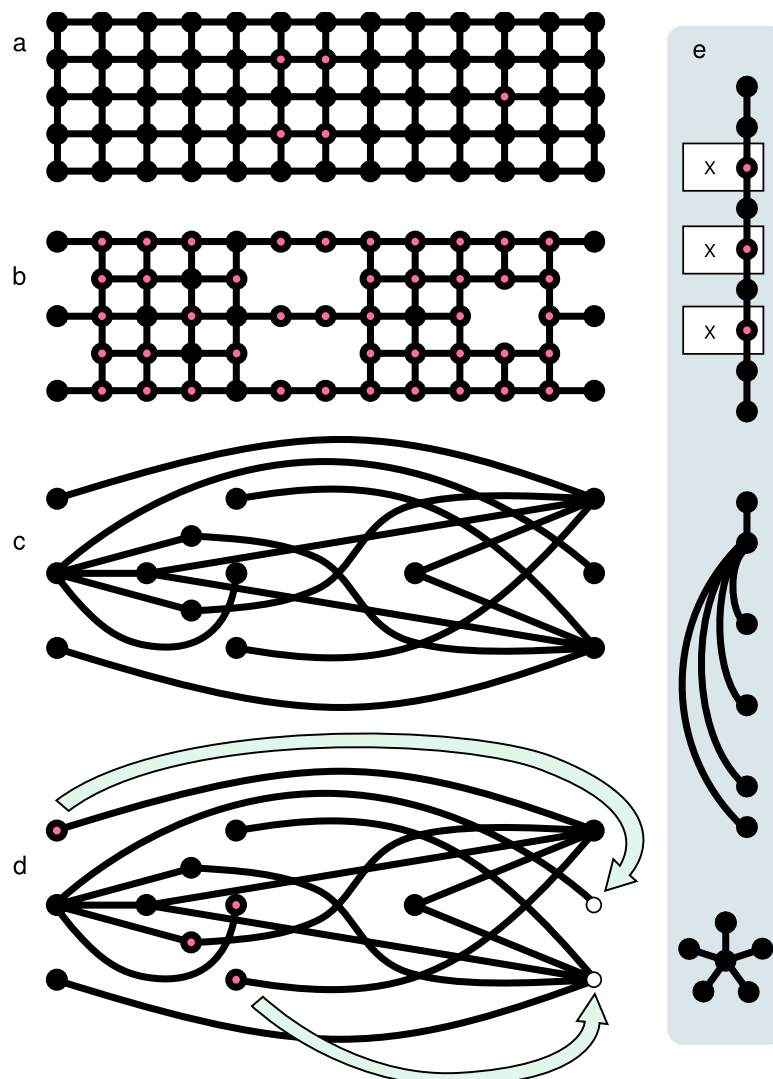


**Figure 2.** Progressive measurement on qubits (marked red). (a) A fully connected cluster state. After Z measurements, (b) and X and Y measurements we obtain an MGS (c) for the algorithm, here a Toffoli gate. In practice one would further reduce the number of qubits required by just in time graph creation—any qubit whose set of edges are complete can be measured and ‘recycled’ to the ‘front’. Right panel (e) indicates the overhead required in the BK scheme in making high degree vertices: one measures out a portion of the qubits (in the X basis here) in order to alter the graph topology.

network  $N_{\text{Basic}}$ . The basic building block can be taken to be a cross shape of length 4, requiring four EPR pairs, and the application of two shifter and one basic networks. One row of width  $n$  can be build using  $2n$  invocations of the shifter network and  $2n$  uses of the basic network. A two-dimensional cluster state on an  $n \times n$  cubic lattice hence requires

$$N_{\text{Shifter}}(n) = 2n^2, \quad N_{\text{Basic}}(n) = 3n^2 - n. \quad (13)$$

## 5. Just in time graph creation

In a lattice system, one may be well advised to prepare the multi-particle cluster state in one step, exploiting a natural nearest-neighbour interaction. However, in a scheme as considered here, there is no motivation to prepare graph edges far in advance of the eventual measurement operations that will consume them. One should therefore avoid doing so since this gives rise to unnecessary errors due to the gradual degradation in phase integrity from decoherence. Instead, one can introduce new edges and vertices for our MGS shortly before it is needed, in a manner analogous to the block-by-block process of [15] but at a finer scale. By analogy to the term used in classical computing, this may be referred to as ‘just in time’ graph-state generation<sup>8</sup> (see also [10, 44]). As noted earlier in section 3, although we may require local unitaries to create the EPR pairs which constitute our ‘raw ingredient’, the remaining steps involved in generating new graph structure can take place without such manipulations.

One can easily confirm that this is possible, even though the measurements on earlier parts of the graph are tilted and therefore have taken the system to a non-graph state. Consider a graph state with graph  $G = (V, E)$  corresponding to the whole computation: let us consider the state vector after  $k$  measurements on vertices  $a_1, \dots, a_k$ , forming a vertex set  $V_k \subset V$ . The resulting state vector after measurements in direction  $r_k$ —depending on the measurement outcomes  $s_1, \dots, s_k \in \{-1, 1\}$ ,—in this temporal order is given by  $P_k|G\rangle = \prod_{j=1}^k (\mathbb{1} + (-1)^{s_j} r_j(s_1, s_2, \dots, s_{j-1}) \sigma^{(a_j)})/2 |G\rangle$ , where  $\sigma^{(a_j)}$  is the vector of Pauli matrices at vertex labelled  $a_j$ . Note that the appropriate measurement basis  $r_j(s_1, s_2, \dots, s_{j-1})$  at step  $j$  depends on the earlier measurement outcomes. Yet, at this point we could have just prepared

$$|G_k\rangle = \prod_{(a,b) \in E_k} P^{(a,b)} |+\rangle^{\otimes n} \quad (14)$$

before performing the above measurements, where  $E_k = \{(a, b) \in E : a \in V_k \text{ or } b \in V_k\}$ . Thus, the only constraint on this just in time approach, is that one should ensure that all edges in  $E_k$  are appropriately entangled in step  $k$ , see figure 2(d).

## 6. Error analysis

A physical implementation of this scheme would be subject to a number of possible errors. Our protocol relies on the subsystems being identical, so that their outputs are indistinguishable. Thus, mismatching parameters will lead to a reduction in performance. Other errors include dephasing of the matter qubits, imperfect optical excitation, phase noise (or drift) in the optical apparatus and photon loss. In this section the majority of our analysis will focus on errors due to mismatched subsystems; we will comment on the other error sources at the end.

<sup>8</sup> An amusing analogy for this approach is provided by the method that prehistoric builders are supposed to have used to transport monolithic stones such as those forming Stonehenge. The stone might be rolled on a set of tree-trunks, as each tree-trunk emerged from behind the stone, it would be quickly brought around the front ‘just in time’ for the stone to roll on to it. Thus they would require only a few tree-trunks rather than paving the entire route with such rollers—a tremendous saving in resources.



Since the results described here involve the detection of two photons arriving from a source, the qualitative effect of errors will be similar to the results presented in [38], and we analyse the system using similar methods. For the purpose of this analysis, we assume that each atom is a three-level system, with degenerate ground states, labelled  $|0\rangle$  and  $|1\rangle$ , and a level  $|e\rangle$  that is optically coupled to  $|1\rangle$ , with an energy  $\hbar\omega_e$ . The cavity is taken to have a frequency  $\omega_c = \omega_e + \Delta$ , where  $\Delta$  is nominally zero. The transition  $|e\rangle \leftrightarrow |1\rangle$  couples to the cavity mode with a strength  $\Omega$ , and the cavity mode decays with a rate  $\Gamma$ . Thus, we consider here imperfections in  $\Delta_j$ ,  $\Omega_j$  and  $\Gamma_j$  for each atom–cavity subsystem,  $j = 1, \dots, 4$ . A comparable analysis was performed in [24], so that we can compare the two-qubit scheme with the present four-qubit protocol. Remarkably, we find that the sensitivity to defects in the apparatus is essentially the same.

### 6.1. Continuous measurement analysis

In the following, we describe the dynamics of a three-level atom in a leaky cavity in the Schrödinger picture, continuously monitored by a photodetector. Its stochastic dynamics under continuous measurement can be described using a quantum-jump approach, leading to a piecewise deterministic classical stochastic process in the set of all pure states [45]–[47]. The continuous time evolution is governed by an effective Hamiltonian, interrupted by discontinuous ‘jumps’ reflecting photon detection. This continuous part is described by the Schrödinger equation  $\partial_t |\tilde{\psi}\rangle = -i\tilde{H}|\tilde{\psi}\rangle$  for the unnormalized state vector  $|\tilde{\psi}\rangle$ , with the non-Hermitian, effective Hamiltonian

$$\tilde{H} = \omega_e |e\rangle\langle e| + (\omega_c - i\Gamma/2) c^\dagger c + \Omega(c|e\rangle\langle g| + c^\dagger |g\rangle\langle e|), \quad (15)$$

where  $c$  is an annihilation operator for the cavity mode. The decreasing vector norm of  $|\tilde{\psi}(t)\rangle$  due to the non-unitary evolution,  $\tilde{U}(t) = e^{-i\tilde{H}t}$ , leads to the cumulative density function for the time at which the photodetector registers a photo-count,

$$P(t) = 1 - |||\tilde{\psi}(t)\rangle||^2. \quad (16)$$

This in turn governs the waiting time distribution in the stochastic process. Correspondingly, a detector click corresponds to a ‘jump’ in the state of the system according to  $|\psi\rangle \mapsto \gamma c|\psi\rangle$ , where  $\gamma = \Gamma^{1/2}$  [45].

For a system of four atoms in cavities, with four detectors following a beam-splitter network, the only change to this prescription is that  $\tilde{U}(t) = \prod_j \tilde{U}_j(t)$  and a click in detector  $k$  effects a ‘jump’ in the state according to  $|\Psi\rangle \mapsto d_k |\Psi\rangle$ , where  $d_k$  is related to the cavity mode operators according to,  $d_k = \sum_j \beta_{k,j} \gamma_j c_j$ , where  $\beta = (\beta_{k,j})$  is the unitary induced by the beam-splitter network. Note that we use  $j = 1, \dots, 4$  to label subsystems and  $k = 1, \dots, 4$  to label detectors.

We examine the effect of errors on the basic 4BS network, which creates four-GHZ states from two EPR pairs, so that the initial state vector is given by  $|\Psi(0)\rangle = |\text{EPR}_{1,2}\rangle |\text{EPR}_{3,4}\rangle$ . We treat the initial excitation of the protocol,  $|1\rangle \rightarrow |e\rangle$ , as instantaneous and ideal, and examine the effect of mismatched system parameters  $\Gamma_j$ ,  $\Delta_j$  and  $\Omega_j$  on the subsequent emission and detection process. The attraction of our protocol is that the initial state is in the two-excitation subspace, so we expect to register exactly two detector counts. The state vector of the system at the end of the protocol is conditional upon which detectors clicked,  $k_1$  and  $k_2$ , and at what times,  $t_1$  and  $t_2 = t_1 + \Delta t$ ,

$$|\tilde{\Psi}(t_1, k_1; t_2, k_2)\rangle = d_{k_2} \tilde{U}(\Delta t) d_{k_1} \tilde{U}(t_1) |\Psi(0)\rangle. \quad (17)$$

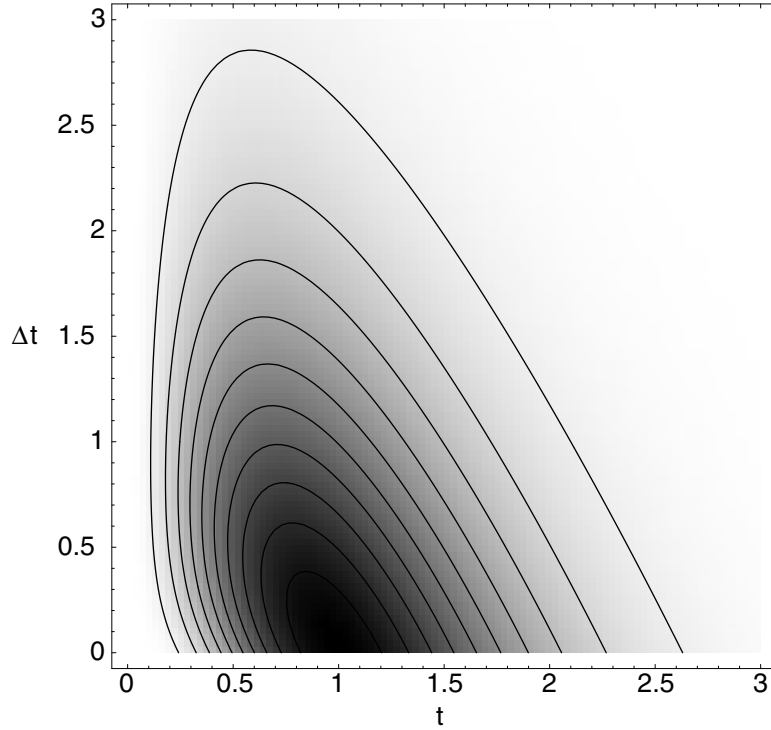


**Figure 3.** Probability density function,  $p(t; \Delta t)$ , for measuring the first photon at time  $t$  followed by the second after a delay of  $\Delta t$ . We have used  $\Omega = 1$ ,  $\Gamma = 4$  and  $\Delta = 0$  for all subsystems.

This particular outcome occurs with a probability density function given by  $p(t_1, k_1; t_2, k_2) = ||\tilde{\Psi}(t_1, k_1; t_2, k_2)||^2$ . Integrating  $p$  over  $t$  and  $\Delta t$  yields the probabilities in table 1, as required. Note that for the ideal case, the distribution of  $p$  does not actually depend on  $k_1$  and  $k_2$ ; the only dependence is an overall multiplicative factor such that table 1 is satisfied. An example is shown in figure 3.

For a given combination of detectors and times, we calculate the fidelity of the resulting state with respect to the ideal outcomes, shown in table 1, which depend only on the detectors and not the times:  $f(t_1, k_1; t_2, k_2) = |\langle \Psi(k_1, k_2) | \Psi(t_1, k_1; t_2, k_2) \rangle|^2$  (note that we have renormalized the state, denoted by the lack of a tilde). In order to give a fair estimate of the expected fidelity, we compute the time-averaged fidelity for outcomes where different detectors click,

$$\begin{aligned}
 F &= 2 \sum_{k_1 \neq k_2} \int_0^\infty dt_1 \int_{t_1}^\infty dt_2 p(t_1, k_1; t_2, k_2) f(t_1, k_1; t_2, k_2) \\
 &= 2 \sum_{k_1 \neq k_2} \int_0^\infty dt_1 \int_{t_1}^\infty dt_2 \tilde{f}(t_1, k_1; t_2, k_2),
 \end{aligned} \tag{18}$$

where  $\tilde{f}(t_1, k_1; t_2, k_2) = |\langle \Psi(k_1, k_2) | \tilde{\Psi}(t_1, k_1; t_2, k_2) \rangle|^2$ , and the factor of 2 accounts for the fact that in the ideal case the probability of fusing the states is 1/2.  $\tilde{f}$  consists of a sum of exponentially decaying terms, so we compute  $F$  analytically, though the expression is rather lengthy.

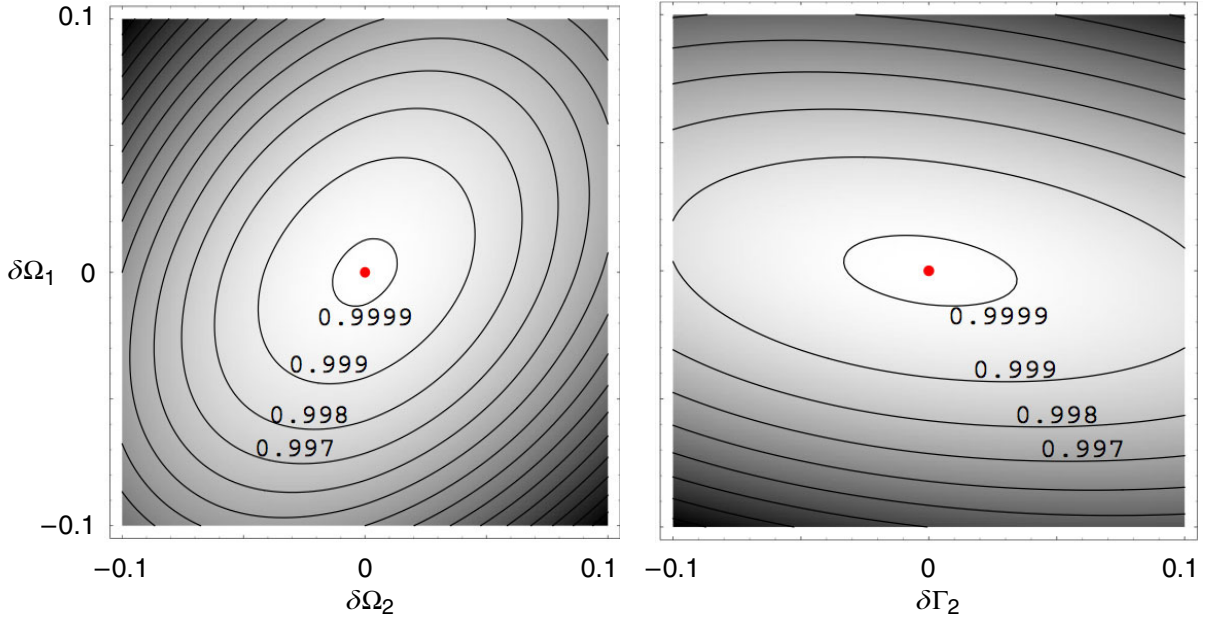


**Figure 4.** Contours of fidelity,  $F$ , as a function of  $\Omega_1 = 1 + \delta\Omega_1$  (vertical axes) and  $\Omega_2 = 1 + \delta\Omega_2$  (left), and  $\Gamma_2 = 4 + \delta\Gamma_2$  (right). All other parameters are fixed at  $\Delta_j = 0$ ,  $\Omega_j = 1$  and  $\Gamma_j = 4$ . The innermost contour is at  $F = 1 - 10^{-4}$  whilst all others are at  $10^{-3}$  intervals.

When  $\Omega_j = \Omega$  and  $\Gamma_j = \Gamma$ , we find  $F = 1$ , so that the protocol works perfectly. Otherwise, the process works with reduced fidelity, as shown in figure 4. Since we are considering three error parameters per subsystem, we cannot show the dependence of  $F$  on all of them graphically; however, for small perturbations to the parameters, we can straightforwardly compute the dependence to quadratic order. In what follows, we work in units for which  $\Omega = 1$ . We find that  $F \approx 1 - \sum_j \epsilon_j^T M_s \epsilon_j - \sum_{j_1 \neq j_2} \epsilon_{j_1}^T M_\times \epsilon_{j_2}$ , where

$$\epsilon_j = (\delta\Delta_j, \delta\Gamma_j, \delta\Omega_j) \quad (19)$$

is the vector of parametric errors in subsystem  $j$  and  $M_{s,\times}$  are the coefficient matrices. For a critically damped atom–cavity system,  $\Gamma = 4\Omega$ , the coefficient matrices are

$$M_s = \begin{bmatrix} \frac{5}{128} & 0 & 0 \\ 0 & \frac{3}{32} & -\frac{3}{16} \\ 0 & -\frac{3}{16} & \frac{9}{16} \end{bmatrix}, \quad M_\times = \begin{bmatrix} -\frac{3}{128} & 0 & 0 \\ 0 & -\frac{1}{32} & \frac{1}{16} \\ 0 & \frac{1}{16} & -\frac{3}{16} \end{bmatrix}. \quad (20)$$

## 6.2. Photon loss

Given an ideal apparatus, without any photon loss or detector failure, our fusion process would merely require four simple non-photon-number-resolving detectors. However, in practice, any

near-future experiment will certainly suffer significant photon loss. This appears potentially very damaging to our scheme (and to that of [25], but not to that of [24]), because we may misinterpret a photon loss as two photons entering a single detector. In order to counter this issue, we would require a limited degree of photon resolution at the detectors—specifically, we must differentiate the three cases: 0, 1 and more than one photons. This suffices to detect a photon loss event—we would then reset the associated matter qubits and rebuild the graph section (analogously to [24]). Importantly, graph-state fidelity will not be affected by undercounts, reflecting a non-unit detection efficiency, which is the dominant problem in real world photon detector technologies. Undercounting is equivalent to a lossy channel followed by a perfect photon counter, and therefore detector inefficiency is simply subsumed into the total photon loss rate. Detector over-counting, i.e. dark counts, are potentially harmful in the present scheme and those of [24, 25]. Fortunately, since we know that correct operation of the scheme generates precisely two photons, we will successfully identify any photon loss event unless the loss occurs at the same time when the detector is independently subjected to a dark count, a process that is expected to happen with a very small probability.

One could construct an adequate detector simply from two non-photon-resolving detectors, together with a fast switch. This would exploit the fact that when two photons are incident on one detector, they are typically separated by a time interval of order  $1/\Gamma$ , see figure 3; this time can be made long enough to trigger a Pockels cell to redirect a possible second photon into a second detector, obviating the need for a true number-resolving detector. On occasions when the two photons occur too close together for the second to be redirected, we simply undercount and assume photon loss has occurred. To summarize, the present scheme is potentially more susceptible to photon loss than the ‘double heralding’ scheme of [24]. However, the issue can be dealt with using detector technologies that remain relatively simple—we do not require high-fidelity photon number resolving detectors in order to generate high-fidelity graph states.

### 6.3. Other errors

This shows that the protocol is most sensitive to errors in the atom–cavity coupling rate, and less sensitive to detuning or the cavity leakage rate (the same hierarchy as observed in [24]). The method used here can be adapted to include dephasing errors, as it was in [38], however it is rather more cumbersome, so for brevity we do not analyse it in detail here. In [38], it was found that dephasing was minimized when  $\Gamma \approx \Omega$ , since such a critically damped system has the shortest lifetime of excitations in the system. It was also noted that dephasing was negligible when  $\Omega$  and  $\Gamma$  are much larger than the dephasing rate. We expect these statements to hold true in this system as well, since the underlying physical processes are the same.

The issue of ‘interferometric instability’ is relevant to any scheme, in which terms in the matter qubit superposition become coupled to the presence/absence of a photon in a given channel. Any phase noise suffered by a photon in transit through the apparatus ultimately can be mapped onto the matter qubits. Fortunately, there has been enormous progress recently in the development of experimental techniques for phase locking, which should prove to be beneficial for a scheme of the proposed type [48]. Imperfect optical excitation can be dealt with by noting that this simply reduces the initial state fidelity, which thus reduces the protocol fidelity by an equal amount.

## 7. Summary

We have described a scheme that unifies some of the desirable features of previous work on matter qubits and graph states. It is able to achieve deterministic growth while using simple static linear optics and a ‘one shot’ excitation. Moreover, the presented scheme obviates the need for continual local operations on qubits during graph growth, which implies a dramatic speedup in many systems. The scheme proves to have properties that make it ideal for creating the most resource efficient form of graph state, the MGS. These MGSs, which form the essential resource for a given quantum computation, without its classically efficiently trackable Clifford-part, typically correspond to graphs with a high maximal vertex degree. For the preparation of such graph states this scheme is particularly suitable. We observe that the use of MGSs is completely compatible with the idea of ‘just in time’ entanglement generation. Our protocol is relatively robust to mismatch in the subsystems, and an accuracy of greater than 1% in the parameters will provide a fidelity of around 0.9999 in the final state. We hope that the scheme presented in this work can contribute to bringing full-scale graph-state quantum computation closer to practical realization.

## Acknowledgments

We would like to thank H J Briegel, D E Browne, W Munro and E Solano for fruitful discussions, and S Barrett, P Kok and M B Plenio for helpful comments on the paper. This work has been supported by the EPSRC (QIP-IRC), the EU (IST-2002-38877), the DFG (Schwerpunktprogramm QIV), the European Research Councils (EURYI) and the Royal Society.

## References

- [1] Nielsen M A and Chuang I L 2000 *Quantum Computation* (Cambridge: Cambridge University Press)
- [2] Schmidt-Kahler F, Häffner H, Riebe M, Gulde S, Lancaster G P T, Deuschle T, Becher C, Roos C F, Eschner J and Blatt R 2003 *Nature* **422** 408
- [3] Leibfried D *et al* 2003 *Nature* **422** 412
- [4] Jelezko F, Gaebel T, Popa I, Gruber A and Wrachtrup J 2004 *Phys. Rev. Lett.* **92** 076401
- [5] Riebe M *et al* 2004 *Nature* **429** 734
- [6] Nazir A, Lovett B, Barrett S, Reina J H and Briggs A 2005 *Phys. Rev. B* **71** 045334
- [7] Knill E, Laflamme R and Milburn G 2001 *Nature* **409** 46
- [8] Eisert J 2005 *Phys. Rev. Lett.* **95** 040502
- Scheel S and Luetkenhaus N 2004 *New J. Phys.* **6** 51
- Knill E 2003 *Phys. Rev. A* **68** 064303
- [9] Raussendorf R and Briegel H J 2001 *Phys. Rev. Lett.* **86** 5188
- [10] Raussendorf R, Browne D E and Briegel H J 2003 *Phys. Rev. A* **68** 022312
- [11] Hein M, Eisert J and Briegel H J 2004 *Phys. Rev. A* **69** 062311
- [12] Walther P, Resch K J, Rudolph T, Schenck E, Weinfurter H, Vedral V, Aspelmeyer M and Zeilinger A 2005 *Nature* **434** 169
- [13] Yoran N and Reznik B 2003 *Phys. Rev. Lett.* **91** 037903
- [14] Nielsen M A 2004 *Phys. Rev. Lett.* **93** 040503
- [15] Browne D E and Rudolph T 2005 *Phys. Rev. Lett.* **95** 010501
- [16] Cabrillo C, Cirac J I, Garchia-Fernandez P and Zoller P 1999 *Phys. Rev. A* **59** 1025
- [17] Bose S, Knight P L, Plenio M B and Vedral V 1999 *Phys. Rev. Lett.* **83** 5158

- [18] Protsenko I E, Reymond G, Schlosser N and Grangier P 2002 *Phys. Rev. A* **66** 062306
- [19] Simon C and Irvine W T M 2003 *Phys. Rev. Lett.* **91** 110405
- [20] Duan L M and Kimble H J 2003 *Phys. Rev. Lett.* **90** 253601
- [21] Browne D E, Plenio M B and Huelga S 2003 *Phys. Rev. Lett.* **91** 067901
- [22] Zou X B and Mathis W 2005 *Phys. Rev. A* **71** 042334
- [23] Legero T, Wilk T, Hennrich M, Rempe G and Kuhn A 2004 *Phys. Rev. Lett.* **93** 070503
- [24] Barrett S D and Kok P 2005 *Phys. Rev. A* **71** 060310 (R)
- [25] Lim Y-L, Beige A and Kwek L C 2005 *Phys. Rev. Lett.* **95** 030505
- [26] Benjamin S C 2005 *Preprint* quant-ph/0504111
- [27] Schlingemann D and Werner R F 2002 *Phys. Rev. A* **65** 012308
- [28] van den Nest M 2005 *PhD Thesis* KU Leuven
- [29] Schlingemann D 2003 *Quant. Inform. Comput.* **3** 431
- [30] Clark S R, Moura Alves C and Jaksch D 2005 *New J. Phys.* **7** 124
- [31] Kay A, Pachos J K and Adams C S 2005 *Preprint* quant-ph/0501166
- [32] Schön C, Solano E, Verstraete F, Cirac J I and Wolf M M 2005 *Preprint* quant-ph/0501096
- [33] <http://www.bell-labs.com/news/1999/november/10/1.html>
- [34] Eisert J, Jacobs K, Papadopoulos P and Plenio M B 2000 *Phys. Rev. A* **62** 052317
- [35] Collins D, Linden N and Popescu S 2001 *Phys. Rev. A* **64** 032302
- [36] Cirac J I, Dür W, Kraus B and Lewenstein M 2001 *Phys. Rev. Lett.* **86** 544
- [37] Svore K M, Terhal B M and DiVincenzo D P 2004 *Preprint* quant-ph/0410047
- [38] Stace T M, Milburn G J and Barnes C H W 2003 *Phys. Rev. B* **67** 085317
- [39] Varnava M, Browne D E and Rudolph T 2005 *Preprint* quant-ph/0507036
- [40] van den Nest M, Dehaene J and De Moor B 2005 *Phys. Rev. A* **71** 062323
- [41] Gross D 2005 *Diploma Thesis* University of Potsdam
- [42] Mhalla M and Perdrix S 2004 *Preprint* quant-ph/0412071
- [43] van den Nest M, Dehaene J and de Moor B 2004 *Phys. Rev. A* **70** 034302
- [44] Danos V, Kashefi E and Panangaden P 2004 *Preprint* quant-ph/0412135
- [45] Gardiner C W and Zoller P 2000 *Quantum Noise* (Heidelberg: Springer)
- [46] Plenio M B and Knight P L 1998 *Rev. Mod. Phys.* **70** 101
- [47] Holevo A S 2001 *Statistical Structure of Quantum Theory* (Heidelberg: Springer)
- [48] Gilchrist A 2005 private communication